

# Formation and characterization of coronene monolayers on HOPG(0001) and MoS<sub>2</sub>(0001): a combined STM/STS and tight-binding study

Karsten Walzer<sup>1</sup>, Michael Sternberg, Michael Hietschold \*

*Institute of Physics, Chemnitz University of Technology, D-09107 Chemnitz, Reichenhainer Strasse 70, Germany*

Received 2 March 1998; accepted for publication 2 July 1998

## Abstract

Ordered monolayers of the highly symmetric organic molecule coronene (C<sub>24</sub>H<sub>12</sub>) have been deposited under ultrahigh vacuum conditions onto several atomically flat surfaces, such as HOPG(0001) and MoS<sub>2</sub>(0001). The adsorbates have been investigated by scanning tunneling microscopy (STM) and scanning tunneling spectroscopy (STS). We were able to achieve submolecular resolution in the STM images, also while doing STS experiments. Reproducible STS characteristics could also be measured. Monolayer adsorbates of coronene on graphite are found to form a commensurate ( $\sqrt{21} \times \sqrt{21}$ )R10.9° superlattice, which is in agreement with LEED data from the literature.

By applying a density-functional tight-binding method we have calculated the electronic structure of the coronene molecule. These calculations of the spatial distribution of the charge densities and the energetic distribution of the electronic orbitals are compared with our STS measurement data. © 1998 Elsevier Science B.V. All rights reserved.

**Keywords:** Coronene; Density functional calculations; Molecular adsorbates; Scanning tunneling microscopy; Scanning tunneling spectroscopy

## 1. Introduction

Molecular semiconductors, such as coronene and other aromatics, phthalocyanines, porphyrins and charge-transfer systems have been widely investigated during the last decades because of their unique electronic and optoelectronic properties. They have been used to set up organic transistors [1], solar cells [2] or information storage systems [3], to mention only a few. In recent times, interest has increased in building molecular wires,

single-electron transistors and other devices from such molecular and supramolecular systems.

However, the basic scanning tunneling microscopy (STM) study of dielectric organic adsorbates, which started with Gimzewski's paper on single copper phthalocyanine molecules [4] and with the breakthrough of Foster and Frommer's STM measurements on adsorbed liquid crystals in 1988 [5], offered a completely new way to investigate the substrate-adsorbate interaction. In the meantime, many organic molecules have been observed by STM under ambient conditions, in liquids and in ultrahigh vacuum (UHV) (for an overview see, e.g., Refs. [6,7]), or under liquid crystal coverage [5,8]. In the case of a rather

\* Corresponding author. Fax: +49 371 531 3077;  
e-mail: hietschold@physik.tu-chemnitz.de

<sup>1</sup> E-mail: walzer@physik.tu-chemnitz.de

immobile adsorbate phase and an atomically flat substrate a molecular resolution of the organic substance can be achieved. Mostly the outer contours of the molecule investigated can be seen, although the intramolecular contrast is often only weak. In some cases,  $\pi$ -electron systems can be clearly distinguished from linear alkane chains [5,8]. However, in general, the chemical contrast in the STM is still an unresolved problem. Local  $I_T(U_T)$  characteristics and CITS (current imaging tunneling spectroscopy) [9] measurements should help in obtaining more detailed chemical information.

One problem while carrying out STS of adsorbate layers is often insufficient stability of the molecular adsorbates, which is caused by the high mobility of the adsorbed molecules on the substrate at room temperature on one side and by distortions caused by the rather strong local electrical field during the STS measurement on the other. Here, one way out is the use of a rather stable adsorbate system, e.g. coronene (for molecular structure see Fig. 1) on a surface such as graphite(0001). This system is a rather good compromise of a stable adsorbate structure (caused by H–H bonds between the molecules) and a weak interaction with the substrate, which occurs only by overlapping  $\pi$ -orbitals. We strive for such a weak substrate–adsorbate interaction to ensure only slightly distorted electron systems of the molecules. Only in this case is a comparison of STM/STS

results with data of simulations for free molecules appropriate.

In this paper, we present the results of coronene adsorption studies by STM experiments and we compare them with LEED and NEXAFS data from the literature [10–12]. Furthermore, we compare the results of our STM experiments with results obtained by density-functional tight-binding (DF–TB) calculations.

## 2. Experimental

All experimental work was carried out under UHV conditions in a two-chamber UHV system with separate analysis chamber and preparation chamber. Pressures were below  $2 \times 10^{-10}$  mbar (both chambers), and below  $1 \times 10^{-9}$  mbar (in the preparation chamber during evaporation), respectively. Substrates were: (1) highly oriented pyrolytic graphite (HOPG, supplied by Advanced Ceramics Corp.), (2) natural molybdenum disulfide, and (3) freshly UHV-cleaned Si(111) $7 \times 7$  surfaces. Both HOPG and MoS<sub>2</sub> were cleaved under ambient conditions, immediately transferred into UHV, and tempered for  $\geq 30$  min at 180°C to desorb atmospheric adsorbates. After this short procedure, these substrates were ready for use. The preparation of the Si(111) surfaces was done by resistive heating at 400°C for 12 h, followed by a repeated short time flash-heating up to 1200°C by current flow directly through the sample. To check the cleanness, LEED imaging of this substrate was done at the end of the preparation. It showed the typical Si(111) $7 \times 7$  surface reconstruction pattern with sharp and narrow spots.

The substance adsorbed onto the substrates was coronene with a purity of 99% (CAS No. 191-07-1, supplied by Aldrich). No further cleaning of the substance was necessary, except of a slow outgassing in UHV for  $> 12$  h at temperatures just below the sublimation temperature. The cleanness of coronene was checked by mass spectroscopy. We chose the disappearance of the H<sub>2</sub>O peak as the criterion for stopping the outgassing process. Sublimation onto the substrates occurred from a tungsten-wire-heated quartz crucible at crucible temperatures of 95–100°C with rates of typically

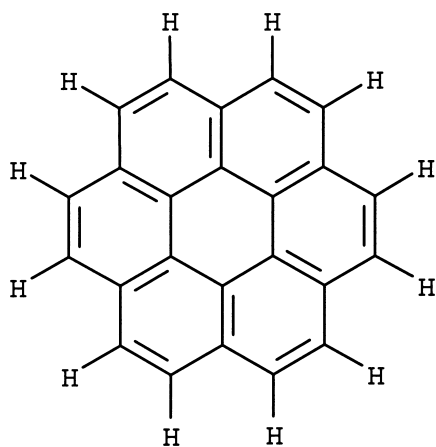


Fig. 1. Structural formula of the coronene molecule.

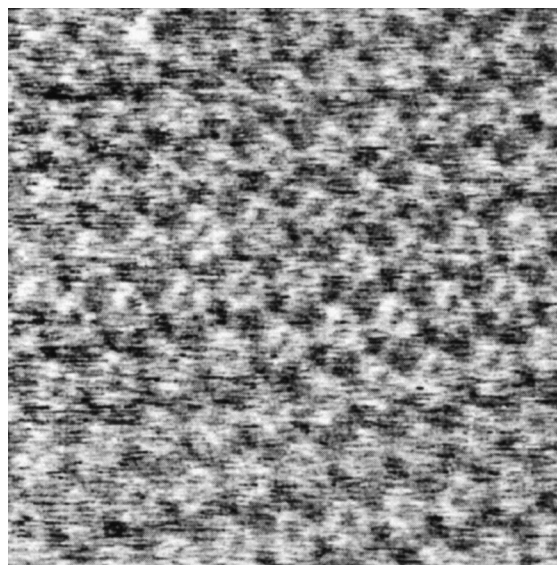
$1\text{--}10\text{ \AA min}^{-1}$ , as measured by a quartz microbalance. In this way adsorbate films with thicknesses of approximately 1 ML were produced.

STM imaging was done at room temperature with a UHV tunneling microscope (Omicron STM-1). All STM images shown in this work were collected in the constant height mode. Electrochemically etched tungsten wires were used as tunnel sensors. They were etched in 2 M NaOH, and after rinsing with distilled water and ethanol immediately transferred into vacuum. For stable tunneling spectroscopy measurements it was important to clean these tips once more in UHV. We did this by frontal argon ion sputtering for 10 min at energies of typically 3 keV, which produces very stable, oxide-free tunnel probes.

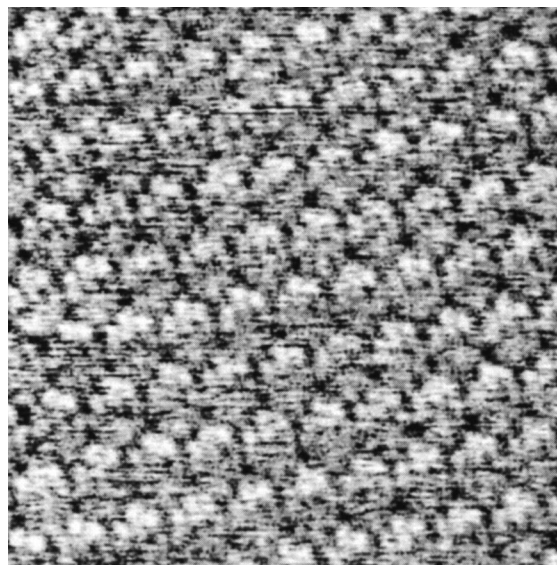
### 3. Results and discussion

#### 3.1. Coronene on graphite (HOPG)

In Fig. 2 we show typical constant height mode STM images of a coronene monolayer on a HOPG(0001) substrate. The molecules are arranged on the substrate surface in a sixfold symmetry with a period of typically  $11 \pm 1\text{ \AA}$ . The internal structure exhibits two different patterns, as shown in Fig. 2a and b: hollow ringlike structures or arrangements of six spots can be observed. Initially we believed these images related to two different molecular orbitals which would be involved in the elastic tunneling process. For evaluation of this hypothesis we carried out some calculations for the molecular orbitals. In Section 4 we will discuss the results of these calculations in detail. To mention the most important point first, we found that STM imaging at low voltages shows only the LUMO or the HOMO, owing to the wide gap in the electronic states of the molecule. Therefore, slight differences in the shape of the molecules' STM images must be due to other reasons, e.g. changes in the electronic configuration at the tip apex or molecules not lying flat. This is presumably the case in Fig. 2b. Because the images of Fig. 2a and b were taken on different samples, slight differences in the layer thicknesses are possible. If we assume a  $>1\text{ ML}$  thickness in Fig. 2b,



(a)



(b)

Fig. 2. (a) Approximately 1 ML of coronene on HOPG, scan-size  $90 \times 90\text{ \AA}^2$ ,  $U_T = 600\text{ mV}$ ,  $I_T = 100\text{ pA}$ . The sixfold symmetry of the adsorbate film is clearly visible. The molecules appear as hollow ring structures. (b) Approximately 1 ML of coronene on HOPG, scan-size  $90 \times 90\text{ \AA}^2$ ,  $U_T = 700\text{ mV}$ ,  $I_T = 100\text{ pA}$ . In this image, in contrast with (a), each molecule appears as an assemblage of six small dots. The molecules are slightly tilted with respect to the substrate plane. Thus, in a constant height mode image, one side of each molecule appears brighter than the other.

the tilted molecules correspond to the NEXAFS results of Yannoulis et al. [12], namely that 1–2 ML of coronene at Ag(111) surfaces grow with a  $16(\pm 10)^\circ$  tilt between substrate and adsorbate. We believe that a comparison of our results with those of Ref. [12] may be done, because both the HOPG(0001) and the Ag(111) surface show a sixfold symmetry and have a low binding energy to the adsorbate. A similar result, however, for thicker layers (100 nm), was obtained McKinnon et al. [13] in their STM experiments. In this work, even more tilted coronene molecules have been found, and the transition to the bulk structure was nearly complete.

Another interesting result of our CITS experiments is the possibility of “tunneling through the molecules” by changing to the typical HOPG tunneling conditions of 2 nA and 0.1 V bias, which exhibits the underlying substrate lattice of the graphite. Fortunately, the centers of the adsorbed molecules remain visible, so we can determine the local adsorption sites directly from these STM images. On the other hand, such long-time stable images of “tunneling through the molecules” may also be taken under conditions that would normally allow an imaging of the pure adsorbate (e.g. 900 mV, 60 pA). One example for such a behavior is shown in Fig. 3. It is interesting that images taken under these conditions seem to be more stable than those taken with graphite tunneling parameters. A similar behavior is also known from other organic systems [14] and it may be accounted for by adsorbed molecules at the tip apex.

A simplified possible explanation could be as sketched in Fig. 4. Fig. 4a shows the energetic conditions of the tunnel contact without adsorbate at the tip. In this case, by applying bias voltages in the range of  $\pm 1$  V the LUMO or HOMO, respectively, of the adsorbed molecules are imaged (case 1 or 3); at voltages of less than  $\pm 100$  mV the graphite substrate becomes visible (case 2). When molecules adsorb onto the tip, the energetic situation of the tunnel contact changes markedly. Again, three cases may be discussed (Fig. 4b). At very low  $|U_T|$  there is no imaging because of the Pauli principle applied to the adsorbed states (case 1). Case 2, tunneling from the HOMO of adsorbed molecules at the tip into graphite states of the

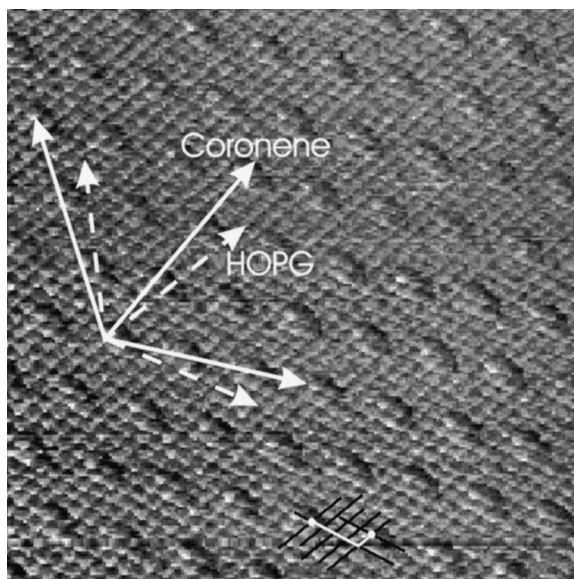


Fig. 3. Simultaneous visibility of adsorbate and HOPG substrate at tunneling conditions of 900 mV and 60 pA setpoint, scansize  $90 \times 90 \text{ \AA}^2$ .

sample, requires voltages in the range of 1 V. These voltages are in the same range as necessary for tunneling in Fig. 4a, case 1. This explains the result that is shown in Fig. 3. The third possibility, tunneling from the HOMO of the tip adsorbate into the LUMO of the sample adsorbate, requires much higher  $U_T$  and may therefore be neglected.

In Fig. 3 it is obvious that there is a shift of the adsorption site by one row of carbon atoms per adsorbed molecule, indicating a  $(\sqrt{21} \times \sqrt{21})R 10.9^\circ$  superlattice for the adsorbed coronene molecules at the HOPG(0001) surface. This is in exact agreement with LEED data from the literature [10]. The resulting adsorption model is sketched in Fig. 5. Here it is interesting that the centers of the molecules are located right above carbon atoms of the substrate as common in graphite. Because of the outer saturation by hydrogen, however, the grids of both carbon structures are twisted relative to each other.

Besides taking STM images the collection of local  $I(U)$  curves was of special interest. All curves were measured with the feedback loop off, at pre-selected tunnel barrier widths<sup>2</sup>. Fig. 6 shows the

<sup>2</sup> The selection was made by choosing an appropriate gap voltage  $U_T$ , the so-called voltage setpoint.

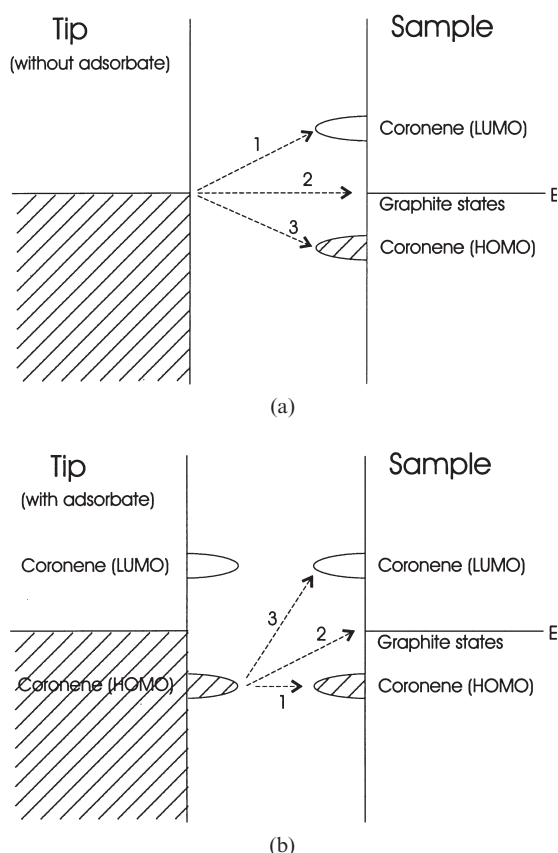


Fig. 4. (a) Energetic conditions at the tunnel gap with grounded clean tip and sample at bias voltage. Three cases occur: (i) imaging of the HOMO of the adsorbate occurs at negative sample bias voltages; (ii) imaging of the graphite states at low bias voltages ( $|U_T| < 100$  mV) and (iii) imaging of the LUMO of the adsorbate at positive sample biases of approximately 1 V. (b) Energetic conditions at the tunnel gap when tip contains adsorbate (tip grounded, sample at positive bias voltage). Again, three cases occur: (i) forbidden; (ii) imaging of the graphite states at voltages of typically 1 V and (iii) imaging of the LUMO of the adsorbate on graphite at voltages of approximately 3 V.

local tunneling spectra of a coronene monolayer on graphite and an uncovered HOPG substrate. As a criterion for the reliability of the collected data, we trusted only those measurements where we were able to obtain stable STM images before and after spectroscopy.

The spectra shown in Fig. 6a were recorded at voltage setpoints of 1260 and 1200 mV for coronene and HOPG, respectively. The coronene

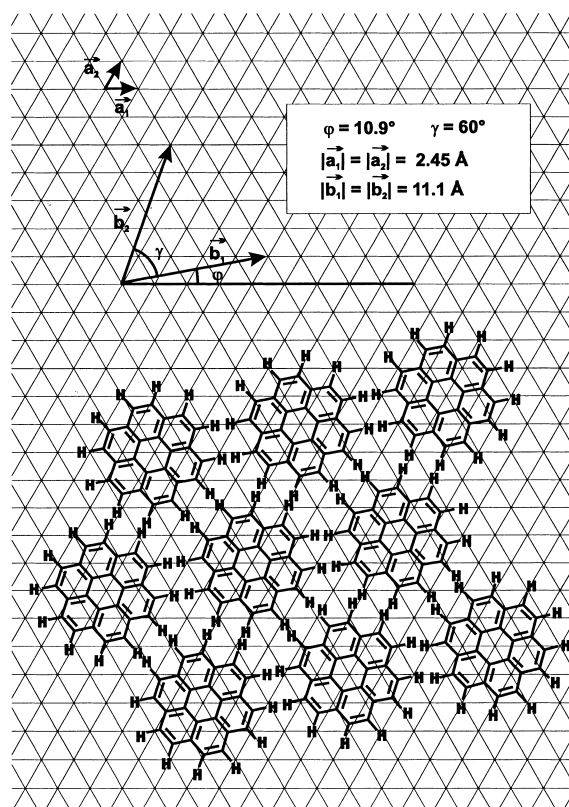


Fig. 5. Model of the adsorption pattern of a coronene monolayer on graphite(0001).

spectrum is a typical spectrum, recorded over the center of a molecule, whereas the graphite spectrum has been averaged over 20 measurements on top of one atom. We chose this method of data presentation, because the collection of a high number of spectra on top of a coronene molecule is difficult owing to the instability of the organic layer in the high electric fields applied for this measurement.

Fig. 6 shows the slightly semiconductive behavior of the samples with a coronene monolayer in the tunnel contact. To speak about a tendency towards a semiconductor is justified, since the  $I(U)$  curves are significantly non-ohmic with  $I_T$  close to zero for several hundred millivolts. The gap width is approximately 1.5 eV, when defined by a tunnel current below 10 pA (resolution limit of the microscope). This gap is much less than the



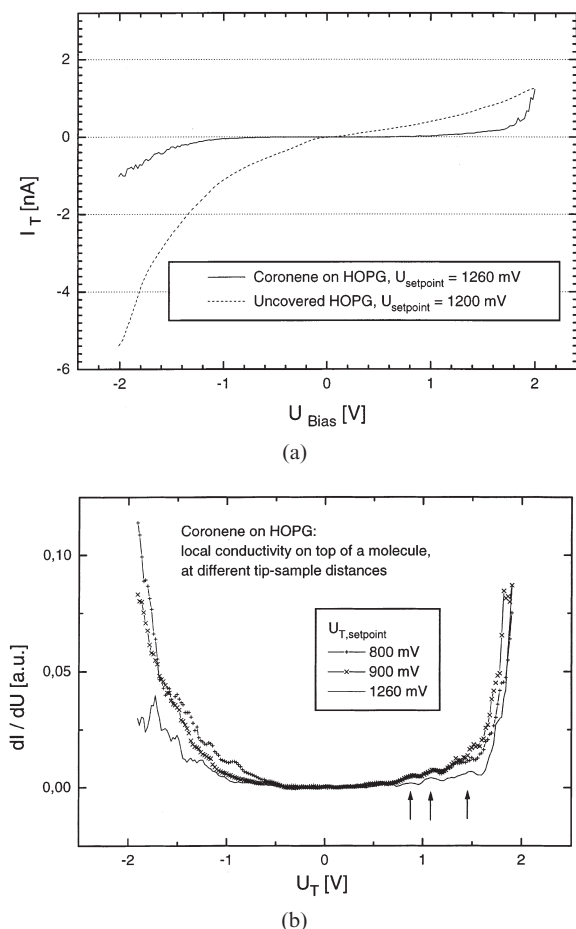


Fig. 6. (a) Tunneling spectra of coronene/HOPG and pure HOPG, collected under similar conditions. (b) Local conductivity spectra of the same coronene/HOPG sample, collected on top of the center of a single molecule at different  $U_T$  setpoints. A widening of the gap with increasing  $U_T$  may be observed. An explanation therefore is the reduced distortion of the tunnel contact by a higher tip-sample distance.

3.0 eV calculated for the free molecule using our DF-TB method, but it cannot be neglected. We explain this narrowing as due to the electronic influences of the substrate and the tip on the energy levels of the coronene molecules. It must be pointed out that an increase of the setpoint voltage at a constant current setpoint (i.e. higher tip-sample distance) leads to a broadening of the measured gap (see Fig. 6b), so the gap becomes closer to the value predicted by the calculations. This behavior may be explained by a reduced

distortion of the sample's states due to a more distant STM probe. Moreover, the  $dI/dU$  curves presented in Fig. 6b show some inner structure, which is reproducible for positive  $U_T$  (marked by arrows in Fig. 6b). An assignment to certain molecular orbitals, however, is not yet possible.

### 3.2. Coronene on $MoS_2(0001)$

This combination shows a rather similar behavior to that for coronene on HOPG(0001): again, we find a sixfold adsorption pattern; see Fig. 7. STM measurements show a lattice constant of  $11 \pm 1$  Å which is the same hcp pattern as on graphite. This provides evidence that the molecule-molecule interactions are predominant with respect to the substrate-adsorbate interaction, as we had supposed in our motivation. Comparisons with literature data from LEED measurements agree with this inference: both Zimmermann et al. [10] and England et al. [11] have found a lattice constant of 11.4 Å, and therefore infer a  $(\sqrt{13} \times \sqrt{13})R13.9^\circ$  superstructure.

It has been observed that coronene adsorbates on  $MoS_2$  are much more sensitive to a distortion by the scanning tip than are the same adsorbate

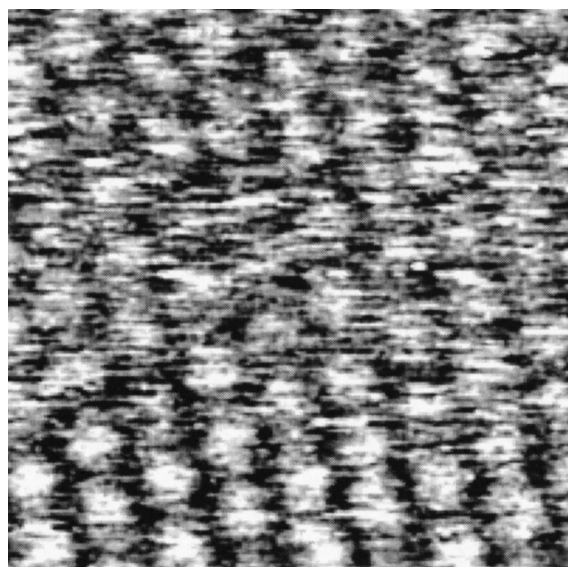


Fig. 7. Coronene adsorbed onto  $MoS_2(0001)$  surface, under approximately monolayer conditions ( $90 \times 90$  Å<sup>2</sup>, 900 mV and 50 pA). No intramolecular resolution could be obtained.

on graphite. Therefore, the STM images of this system are much more noisy and show a short lifetime of only 2–5 STM scans. The reason for this behavior must be seen in the strong lattice mismatch of coronene and  $\text{MoS}_2$  which reduces the binding possibilities of the molecule to the substrate.

### 3.3. Coronene on $\text{Si}(111)7 \times 7$

Coronene was also adsorbed onto the  $\text{Si}(111)7 \times 7$  surface. In contrast to the adsorption of coronene on the  $\text{Si}(100)(2 \times 1)$  surface, where single coronene molecules have been observed by STM [15], on  $\text{Si}(111)$  the higher chemical reactivity of the substrate leads to a destruction of the molecules and results in a distorted silicon surface. This could be observed in STM as a disturbed  $\text{Si}(111)7 \times 7$  reconstructed surface.

## 4. Density-functional tight-binding simulations and comparison with the STM results

In order to attain a better understanding of our STM images we have applied a density-functional-based tight-binding formalism to simulate the coronene molecules and their interaction with the graphite surface.

In contrast to conventional tight-binding schemes where hopping and overlap integrals and their scaling functions are fitted to certain reference structures, in our scheme the atomic basis functions as well as the hopping and overlap integrals as a function of distance are obtained numerically in a largely parameter-free way from a self-consistent calculation of isolated atoms in a parabolic embedding potential. The important feature for STM-related studies is the availability of realistic wave functions which allow the calculation of charge densities at various energies at a given location in the model. The method and its application has been described in great detail elsewhere [16].

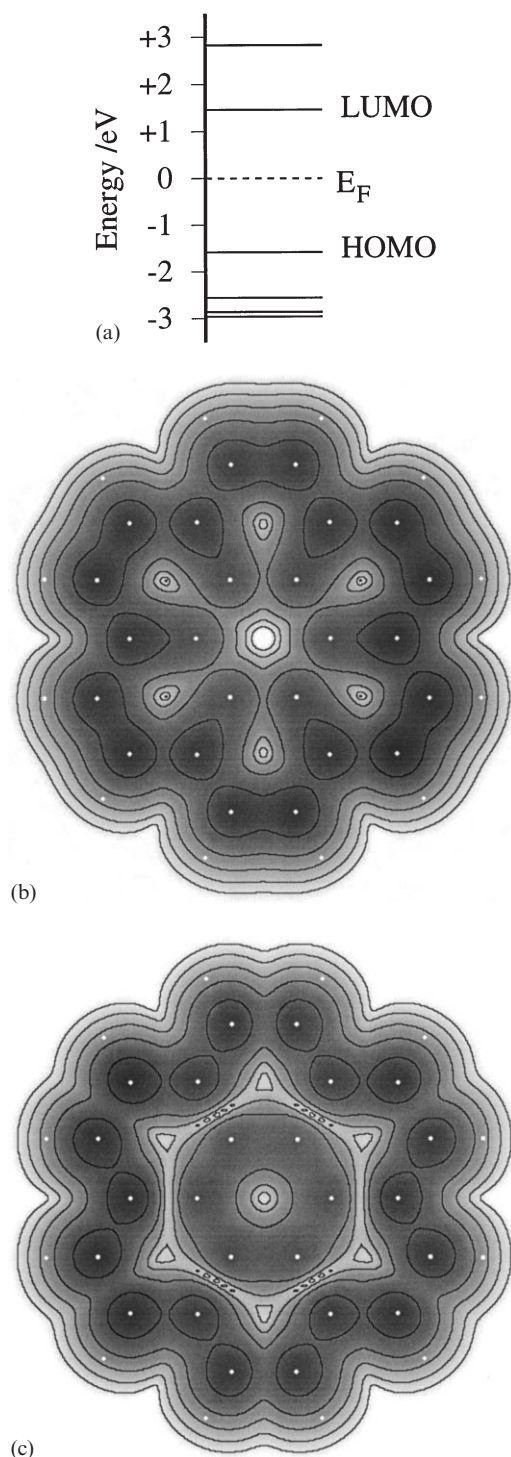
In a first step, an isolated coronene molecule was constructed and relaxed to its lowest-energy configuration. The molecule remains flat and the bond lengths agree within 1–2% with experimental

and other theoretical values. Then we placed the molecule at varying distances and sites above a graphitic slab. No clear energy minimum could be obtained, indicating that the adsorption of coronene molecules on graphite is not due to covalent bonding but instead arises from van der Waals forces which are beyond the scope of the DF–TB scheme. The electronic structure of adsorbed coronene should therefore be almost undisturbed compared with that of an isolated molecule. In the following, we discuss the charge density around an isolated coronene molecule and relate it to the observed STM images. Thus, we use an isolated coronene molecule for the purpose of calculating the local charge density on a plane parallel to the molecule. In the Tersoff–Hamann approximation [17] this can be directly interpreted as the quantity imaged by a constant-height STM.

Fig. 8a shows the DF–TB energy levels of coronene near the Fermi energy. We obtain a HOMO–LUMO gap of 3.0 eV. This is in good agreement with the measured gap width of clearly more than 2 eV, mostly 2.5 eV. The difference between the model and the experimental result may be caused by the fact that the model has been calculated for free molecules with neither molecule–molecule nor molecule–substrate interactions. The relatively large gap of coronene agrees with the clearly semiconductive behavior of coronene during STM, and it explains the fact that STM imaging of the metallic graphite substrate at low bias voltages can be done easily “through” the adsorbed molecules. At low tunneling voltages near the Fermi level of graphite we find no coronene states which are involved in the tunneling process. Conversely, when the tunneling voltage coincides with a coronene level, the constant-height image will be dominated by adsorbate states.

In the case of the  $\text{MoS}_2$  substrate a gap of 1.45 eV occurs, such that the HOMO and the LUMO of the adsorbed coronene are closer to the respective band edges of the substrate, which results in difficulties in imaging coronene on  $\text{MoS}_2$ .

The calculation shows that in the isolated coronene molecule the HOMO and the LUMO are energetically clearly separated from lower occupied states and higher unoccupied states by 1.0 eV and



1.4 eV, respectively (Fig. 8a). These large separations indicate that these states alone are the imaging states for a voltage setpoint at one of the corresponding energy levels. Fig. 8b and c show the HOMO and LUMO charge densities, respectively, on a plane located 1.06 Å above the molecular base plane. In both cases the charge density maxima occur mostly above the ring of outermost carbon atoms of the coronene molecule, forming a characteristically sixfold kinked ring structure. The hydrogen atoms are not associated with notable features in the image. For comparison with STM images it is important that there are no significant differences between HOMO and LUMO charge density distribution. Both are more or less ring-shaped with the maximum charge density within the outer ring as it may be seen in Fig. 2a and b. Also the six-spot pattern, which is shown in Fig. 2b can be explained by the results of the calculation.

## 5. Summary

We have studied the adsorption behavior of coronene on three different atomically flat substrates: HOPG(0001), MoS<sub>2</sub>(0001) and Si(111). Molecularly and submolecularly resolved STM images of well-ordered adsorbates could be obtained on both layered material substrates, whereas on Si(111), because of its highly reactive dangling bonds, no preparation of an ordered and undestroyed coronene film was possible. STS measurements on top of coronene molecules adsorbed on graphite resulted in stable curves, if the tip-sample distance was kept in a certain range. The intramolecular resolution of coronene on graphite allows an assignment of the observed molecular images to the lowest unoccupied molecular orbital

Fig. 8. (a) DF-TB energy levels of coronene near the Fermi energy. A HOMO-LUMO gap of 3.0 eV is obtained. (b) HOMO charge density on a plane located 2.0 Bohr radii above the molecular base plane. The grayscale covers three orders of magnitude at a logarithmic scale with a maximum value of  $2.3 \times 10^{-2}$  electrons per Å<sup>3</sup>. (c) LUMO charge density as calculated with the same parameters, same grayscale.



as calculated, although they have been calculated for single, non-adsorbed coronene molecules.

### Acknowledgements

We gratefully acknowledge financial support by Deutsche Forschungsgemeinschaft (Innovationskolleg INK2 “Methods and materials systems for the nanometer range”, subproject B3).

### References

- [1] Y.-Y. Lin, D.J. Gundlach, S.F. Nelson, T.N. Jackson, *IEEE Electron. Device Lett.* 18 (1997) 606.
- [2] R. Takeuchi, M. Takeuchi, *Jpn. J. Appl. Phys.* 36 (1997) L127.
- [3] J. Friedrich, D. Haarer, *Angew. Chem.* 96 (1984) 96.
- [4] J.K. Gimzewski, E. Stoll, R.R. Schlittler, *Surf. Sci.* 181 (1987) 267.
- [5] J.S. Foster, J.E. Frommer, *Nature* 333 (1988) 542.
- [6] J.E. Frommer, *Angew. Chem. Int. Ed. Engl.* 31 (1992) 1298.
- [7] R. Wiesendanger, *Scanning Probe Microscopy and Spectroscopy*, Cambridge University Press, Cambridge, 1994.
- [8] K. Walzer, M. Hietschold, *J. Vac. Sci. Technol. B* 14 (1996) 1461.
- [9] R.J. Hamers, R.M. Tromp, J.E. Demuth, *Phys. Rev. Lett.* 56 (1986) 1972.
- [10] U. Zimmermann, N. Karl, *Surf. Sci.* 268 (1992) 296.
- [11] C.D. England, G.E. Collins, T.J. Schuerlein, N.R. Armstrong, *Langmuir* 10 (1994) 2748.
- [12] P. Yannoulis, R. Dudde, K.H. Frank, E.E. Koch, *Surf. Sci.* 189/190 (1987) 519.
- [13] A.W. McKinnon, M.E. Welland, St.J. Dixon Warren, *Thin Solid Films* 257 (1995) 63.
- [14] A. Quivy, R. Deltour, P.J.M. van Bentum, J.W. Gerritsen, A.G.M. Jansen, P. Wyder, *Surf. Sci.* 325 (1995) 185.
- [15] Y. Maeda, T. Matsumoto, T. Kawai, *Surf. Sci.* 384 (1997) L896.
- [16] M. Sternberg, Th. Frauenheim, W. Zimmermann-Edling, H.G. Busmann, *Surf. Sci.* 370 (1997) 232.
- [17] J. Tersoff, D.R. Hamann, *Phys. Rev. B* 31 (1985) 805.